
This is an electronic reprint of the original article.
This reprint may differ from the original in pagination and typographic detail.

Khadka, Ambika; Kokkonen, Teemu; Koivusalo, Harri; Niemi, Tero J.; Leskinen, Piia; Körber, Jan Hendrik

Stormflow against streamflow – Can LID-provided storage capacity ensure performance efficiency and maintenance of pre-development flow regime?

Published in:
Journal of Hydrology

DOI:
[10.1016/j.jhydrol.2021.126768](https://doi.org/10.1016/j.jhydrol.2021.126768)

Published: 01/11/2021

Document Version
Publisher's PDF, also known as Version of record

Published under the following license:
CC BY

Please cite the original version:
Khadka, A., Kokkonen, T., Koivusalo, H., Niemi, T. J., Leskinen, P., & Körber, J. H. (2021). Stormflow against streamflow – Can LID-provided storage capacity ensure performance efficiency and maintenance of pre-development flow regime? *Journal of Hydrology*, 602, Article 126768.
<https://doi.org/10.1016/j.jhydrol.2021.126768>

This material is protected by copyright and other intellectual property rights, and duplication or sale of all or part of any of the repository collections is not permitted, except that material may be duplicated by you for your research use or educational purposes in electronic or print form. You must obtain permission for any other use. Electronic or print copies may not be offered, whether for sale or otherwise to anyone who is not an authorised user.



Research papers

Stormflow against streamflow – Can LID-provided storage capacity ensure performance efficiency and maintenance of pre-development flow regime?

Ambika Khadka^{a,*}, Teemu Kokkonen^a, Harri Koivusalo^a, Tero J. Niemi^b, Piia Leskinen^c, Jan-Hendrik Körber^c

^a Department of Built Environment, School of Engineering, Aalto University, Finland

^b Finnish Meteorological Institute, Helsinki, Finland

^c Turku University of Applied Sciences, Turku, Finland



ARTICLE INFO

This manuscript was handled by Sally Elizabeth Thompson, Editor-in-Chief

Keywords:

Storage capacity
Pre-development flow regime
Performance efficiency

ABSTRACT

The goal of Low Impact Development (LID) is to restore and maintain the pre-development flow regime. The static storage capacity, which is often used as a parameter in LID designs, provides the maximum capacity of an LID type and is easily quantifiable already at the design phase. However, the static storage approach does not consider the inter-event recovery of storage capacity by infiltration and evapotranspiration. This study investigated dynamic storage capacities of three stormwater management designs with increasing proportions of LID units on a 1.2 ha urban residential block in Southern Finland, to compare their cost-efficiency, as well as their potential in restoring the pre-development flow regime. The cost-efficiency of LID designs was assessed based on their ability to contribute to water losses, and on the additional construction costs required when comparing them to conventional solutions (e.g. asphalt replaced with permeable pavement). The design with a small storage capacity and a large capture ratio, i.e., the ratio of contributing area to LID area, was the least efficient albeit its small construction cost. The design with an appropriate balance between the capture ratio and the LID provided storage capacity was the most efficient option. In assessing the potential of stormwater designs in restoring the pre-development flow regime, the sum of infiltration and flow in storm sewer networks was more representative of the catchment total runoff than flow alone. Finally, an extensive simulation of a large set of differently placed LID units proved useful in a priori identification of the most influential units in the treatment train.

1. Introduction

Urbanized catchments with a large fraction of impervious cover drastically disrupt the natural flow dynamics compared with undisturbed catchments (Guan et al., 2015b; Sillanpää, 2013). The hydrological impacts of urbanization have globally become a major management concern for cities. Motivation for stormwater management is the need to restore a part of those natural hydrological functions that were lost by construction of impervious and nearly impervious surfaces and efficient stormwater drainage and conveyance systems. Accordingly, there is an increasing interest towards economically and hydrologically efficient approaches to manage stormflow with low impact development (LID) solutions.

LID types that enhance infiltration, evapotranspiration, and storage of stormwater have become increasingly popular in landscape-architectural designs and urban planning due to their potential to

mimic natural hydrological processes. The current design guidelines for LID types are mostly based on the static storage capacity, i.e., surface storage volume and soil media void space volume, which are dimensioned according to the rainfall intensity for a design storm or a short-term event (Ebrahimian et al., 2019). In areas where precipitation intensities are moderate and back-to-back storms are rare, this approach may lead to over dimensioning of LID systems (Traver and Ebrahimian, 2017). Although the benefits of LID-provided static storage capacity in reducing peak flows and volumes of stormflow have been studied (Haghighatafshar et al., 2018; Walsh et al., 2014), the role of stormwater losses during inter-event dry periods in restoring the capacity of LID systems to store stormwater for the next rainfall event has received limited attention. Accordingly, there is a need for continuous simulation of LID systems to assess the role of stormwater losses via dynamic processes, i.e., infiltration and evapotranspiration. Landscape architectural design procedure would benefit from hydrological information that is

* Corresponding author.

E-mail address: ambika.khadka@aalto.fi (A. Khadka).

<https://doi.org/10.1016/j.jhydrol.2021.126768>

Received 18 June 2020; Received in revised form 26 July 2021; Accepted 28 July 2021

Available online 3 August 2021

0022-1694/© 2021 The Author(s). Published by Elsevier B.V. This is an open access article under the CC BY license (<http://creativecommons.org/licenses/by/4.0/>).

rarely available for a design site but can be produced with stormwater models to support design of various LID alternatives.

A substantial body of research has focused on short-term hydrological performance at an individual LID level (e.g. Jia et al. 2012; Qin et al., 2013) or for a combination of LID types (e.g. Guan et al., 2015a; Haghghatafshar et al., 2018). Optimization studies to assess the cost efficiency of individual LID units based on design storms also exist (e.g. Jia et al., 2012; Chui et al. 2016). However, stormwater management designs, which involve several different LID types arranged in a treatment train, can be particularly efficient for newly developed areas where design of LID networks can be included already in the development plan (Jefferson et al., 2017). The combinations of LID types have been reported to be economically and hydrologically more efficient than individual LID types (e.g. Joksimovic & Alam, 2014; Leimgruber et al., 2019). However, understanding the mechanisms that enable serially connected LID types to achieve better economic benefits compared to individual types have received limited attention. Evidently, a model-based assessment of design alternatives is an attractive option to quantify the mechanisms and compare the hydrological and cost performance of the solutions. Modelling also offers the means to generate a large set of LID design alternatives to reveal where the key LID units are located in the treatment train.

This study was motivated by the need to explore the extent to which a range of LID designs can control urban water balance and restore natural behaviour of an urban constructed area. The study explores how long-term dynamic evolution of the LID-provided storage controls water losses and stormwater generation at a block scale, and what the relationship between LID performance and their construction costs is across design alternatives. The assessment was based on a model-based analysis of LID designs that were outlined by a landscape architect, and on a large set of automatically generated LID combinations. The modelling application was targeted into an urban block for detecting LID performance and constructions costs in detail. In addition, the response of urban catchment to rainfall for alternative stormwater management designs was compared against available measured runoff depths from rural watersheds within the study region. The simulations were carried

out for summer (May to August) and autumn (September to November) periods to detect seasonal differences in the performance of alternative stormwater management designs.

The study objectives were:

1) To evaluate static and dynamic storage provided by LID designs and reveal the role of storage recovery during summer and autumn periods with changing evaporative losses.

2) To quantify LID impacts on stormwater losses for alternative designs, and to assess the potential of urban stormwater management designs in restoring the natural runoff regime.

3) To explore relationship between hydrological performance and construction costs of LID designs using a large set of automatically generated combinations of LID types.

2. Materials and methods

2.1. Site description and data

The study area is located at the southwestern coast of Finland (Fig. 1c) comprising three sites with different land use distributions and scales ranging from one hectare to hundreds of square kilometers.

The urban Kirstinpuisto site (14.8 ha) is located in the City of Turku at the border of Kuninkoja and Aurajoki watersheds (Fig. 1a-b). Although the Kirstinpuisto site comprises two catchments with separate stormwater drainage outlets, it will be referred as the Kirstinpuisto catchment hereafter (Fig. 1a). Rainfall data at a one-minute resolution from the city of Turku operated weather station 1.5 km northeast of the Kirstinpuisto catchment was available for a seven-month period from May to November 2012 (Table 1). The summer period from May to August (P1) ended with an intensive rain event having a return period of ca. 100 years. The autumn period from September to November (P2) included another significant rain event with a return period of ca. 30 years.

Outlets of a rural stream Savijoki and a semi-urban stream Kuninkoja define the reference watersheds (Fig. 1b). Savijoki is a tributary of the Aurajoki river (Fig. 1b). The Savijoki watershed has an area of 130 km²,

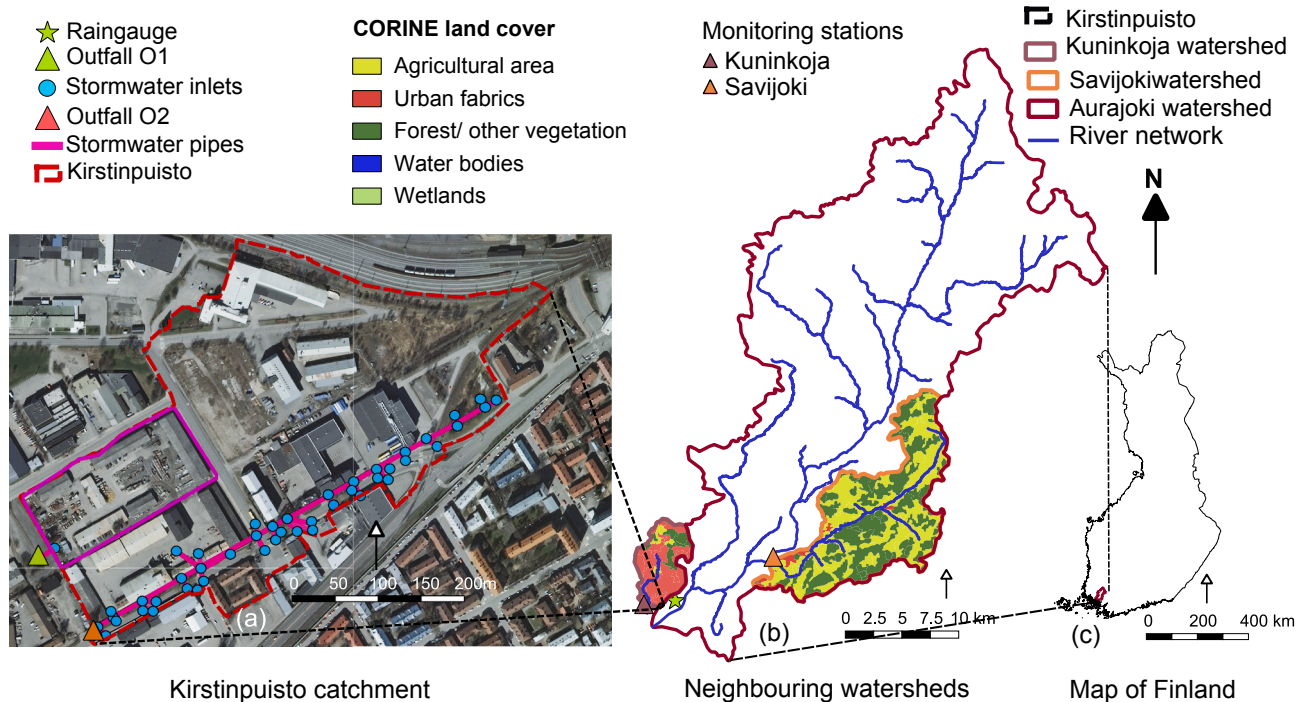


Fig. 1. The study area consisting of Kirstinpuisto catchment (a), and two reference watersheds Kuninkoja and Savijoki (b). Map of Finland is shown in (c). The land cover in (b) is based on CORINE (2018). The purple rectangle within (a) represent the residential block extracted from Kirstinpuisto catchment for detailed analysis. (For interpretation of the references to colour in this figure legend, the reader is referred to the web version of this article.)

Table 1
Measured summer and autumn rainfall and runoff depths, and peak rainfall in 2012.

Period	Duration	Rainfall depth (mm)	Peak rain intensity (mm/10 min)	Runoff depth (mm)	
		Turku		Savijoki	Kuninkoja
P1	May – Aug	286	18.0	19	54
P2	Sept – Nov	164	9.0	118	112

50% of which is covered by agricultural land, 46% by forest and other vegetation, and the remaining 3% by urban fabrics (CORINE, 2018). The total imperviousness of Savijoki watershed is <1% (EEA, 2018). The discharge data for the rural Savijoki watershed was obtained from the stream monitoring station operated by the Finnish Environment Institute (Table 1, Fig. 1b). Kuninkoja is a semi-urban watershed with an area of 33 km². Urban fabrics cover 68% of the watershed area, forest and urban greens 26% of the area, and the remaining 6% is agricultural land (CORINE, 2018). The total imperviousness of Kuninkoja is 24%. The discharge data for the semi-urban Kuninkoja watershed was obtained from the monitoring station operated by the Turku University of Applied Sciences (Table 1, Fig. 1b).

2.2. SWMM parameterization

The Stormwater Management Model (SWMM) (Rossman and Huber, 2016) is a widely used tool to simulate urban water balance components, i.e., surface runoff, flooding, infiltration, and evapotranspiration (Avellaneda et al., 2017; Khadka et al., 2019). The model can also simulate LID structures, where each LID type is represented with a combination of vertical layers such as surface layer or pavement, soil layer, and storage layer (Fig. 2). Parameterization of the three alternative stormwater management designs with an increasing intensity of LID

units was based on a previously calibrated SWMM model for the Kirstinpuisto catchment. The calibrated imperviousness fraction, Manning's roughness, and depression storage parameters for paved surface, gravelled surface, roofs and train tracks used in this study can be found in Table 4 in Khadka et al. (2019). Infiltration was modelled using the Green-Ampt equation. For LID types with vertical layers (Fig. 2), the water lost from the storage layer to the underlying soil layer forms the infiltration component in the water balance. The exchange of groundwater with the drainage network was not modelled. The initial moisture condition at the beginning of P1 was considered to be equal to the wilting point moisture content of the soil layer whereas the initial condition for P2 was set according to the end-of-period storage values of P1.

The vegetated areas within the Kirstinpuisto catchment were parameterized with the aim to realistically produce the division of losses into evapotranspiration and infiltration. The existing vegetation in the Kirstinpuisto catchment was described as a rain garden with a 60% vegetation coverage on a 60 cm of underlying clay soil, and a 3 cm surface layer to represent urban herbaceous plants (Tahvonen, 2018). Manning's roughness of the surface layer and infiltration parameters of the Green-Ampt equation, i.e., hydraulic conductivity, conductivity slope and suction head of the soil layer (Table 2), were adjusted so that the simulated green area evapotranspiration values match with values reported for agricultural and peatland forest catchments in Turunen (2017) and Sarkkola et al. (2013).

A residential block of 1.2 ha was extracted from the Kirstinpuisto catchment for a detailed analysis of the stormwater management designs at the block scale (Figs. 2 and 3). The block offers a computationally economic way to evaluate the performance of LID types arranged in a treatment train without the need to simulate the entire catchment. An urban area can be considered as a collection of blocks so examining the hydrological behaviour of one block yields results that are indicative of the behaviour of a larger urban development.

In design A, the block consisted of six 4–6 storey apartment

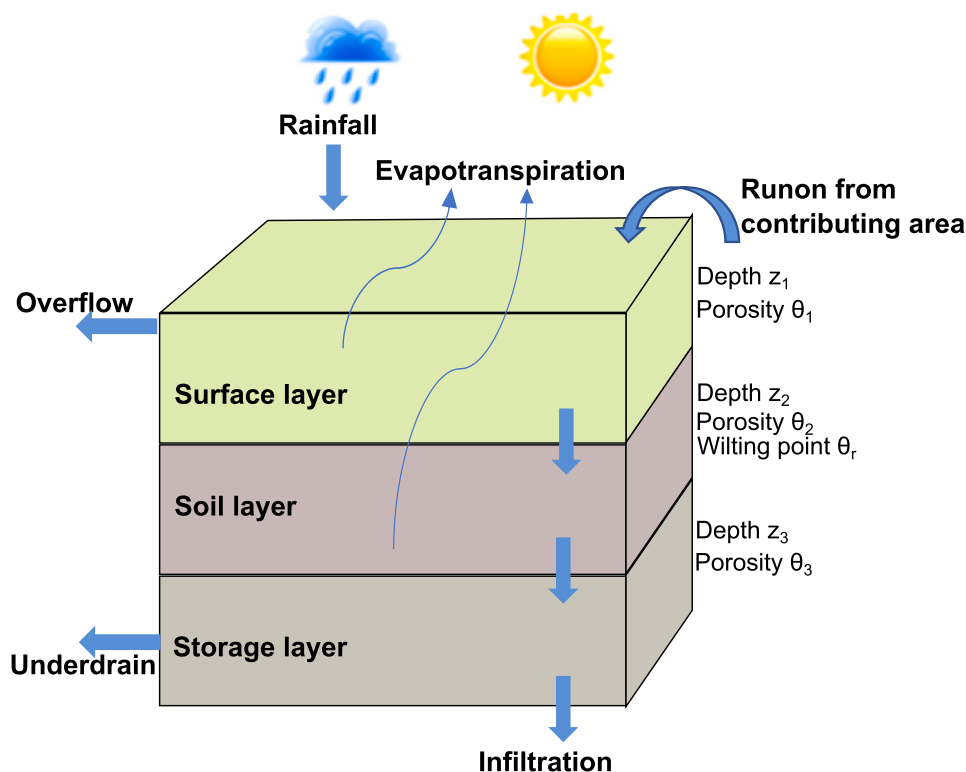


Fig. 2. Generic illustration of an LID technique. Not all layers are present in all LID techniques. Specific parameter values for vertical layers in LID techniques can be found in Table 3 in Khadka et al. (2019).

Table 2
Parameters used to represent vegetated area.

Surface layer		Soil layer			
Manning's roughness (-)	Vegetative fraction (-)	Thickness (mm)	Conductivity (mm/hr)	Suction (mm)	Conductivity slope (-)
0.7	0.6	600	4.3	208.8	15

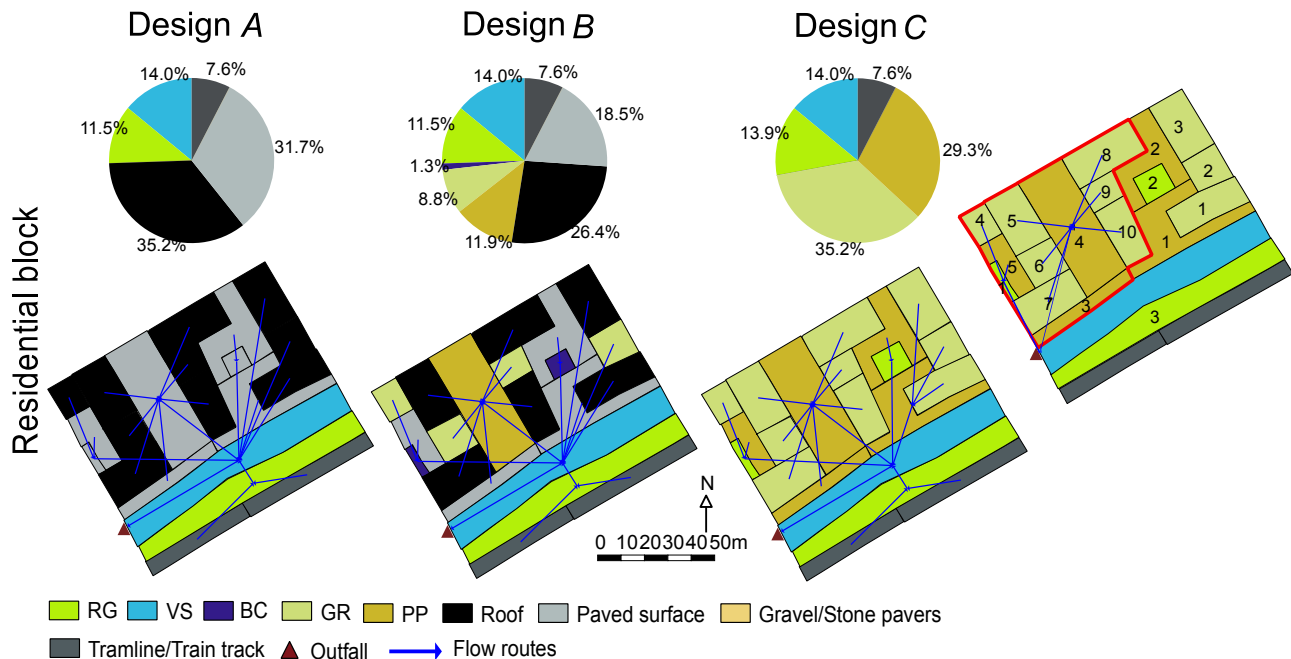


Fig. 3. Stormwater management designs A-C at a residential block. VS, RG, BC, GR and PP refer to vegetated swale, rain garden, bioretention cell, green roof and permeable pavement, respectively. Pie charts show the proportions of different surface types within the studied designs. The red boundary shows the area for the LID activation/deactivation sampling in sensitivity analysis. (For interpretation of the references to colour in this figure legend, the reader is referred to the web version of this article.)

buildings, stone-paved yards and an asphalt parking space adjacent to green elements, i.e., a vegetated swale and a rain garden (Fig. 3). In stormwater management designs B and C, more LID types were added to supplement the vegetated swale of design A.

2.3. LID cost estimation

The investment costs, including materials and works, of each LID type (Table 3) were estimated according to German design guidelines (DWA, 2014), cost estimation frameworks (Manfred, 2012) and implementation guidelines for LID types (Behörde für Stadtentwicklung und Umwelt Freie und Hansestadt Hamburg, 2006). These sources consider design and construction requirements set by the German Institute for Standardization.

In a newly developed area, either an LID type or its conventional counterpart can be implemented, i.e., a permeable pavement or a bioretention cell instead of asphalt, and a green roof instead of a conventional flat roof. However, the property developers are still hesitant to choose LID types over conventional solutions due to their concerns for higher initial investment costs and uncertain efficiencies. Thus, this study estimated the cost of LID types per unit area as the additional cost

Table 3
Investment cost estimates for different LID types.

LID	Rain garden (RG)	Vegetative swale (VS)	Bioretention cell (BC)	Permeable pavement (PP)	Green roof (GR)
Cost €/m ²	20*	38	75*	45*	30**

* Additional costs compared to asphalt.

** Added cost for extensive GR compared to conventional flat roof.

of implementing LID types instead of their conventional counterparts based on initial investment costs (Table 3). Operational and maintenance costs were excluded from the cost estimation as they are highly site specific, and poorly transferable to other regions. The cost of underlying land was also ignored as it would not affect the cost difference between LID and conventional structures. The cost difference between an LID type and a conventional solution is referred to as investment cost hereafter.

2.4. Performance evaluation

2.4.1. Storage capacity and dynamics

Stormwater management designs A-C were assessed for their maximum capacity to store stormwater in LID structures. Storage capacity (M_{tot}) was computed using Eqs. (1)–(3) based on the physical characteristics of the vertical layers in each LID type (Fig. 2):

$$D_i = z_1\theta_1 + z_2(\theta_2 - \theta_r) + z_3\theta_3 \tag{1}$$

$$M_i = D_i \frac{A_i}{A} \tag{2}$$

$$M_{tot} = \sum_{i=1}^n M_i \quad (3)$$

where D_i is the storage depth of an LID type i in water column depth [mm], z_1 , z_2 and z_3 are the depths of surface, soil and storage layers [mm], respectively, θ_1 , θ_2 and θ_3 are the porosities of the surface, soil and storage layers [-], θ_s is the wilting point in the soil layer [-], M_i is the LID specific storage capacity for an LID type i for the residential block [mm], A_i is the surface area of an LID type i [m²], A is the total surface area of the residential block [m²], and n is the total number of LID types.

In order to present the dynamic aspect of the LID specific storage capacity, the time series and the exceedance frequency of storage in LID types during the 7-month simulation period for designs A-C were visualised. Depth of stormwater stored in an LID type i at time t ($S_{i,t}$) was computed from the simulated water balance components as follows:

$$S_{i,t} = [S_{i,t-1} + \Delta t(F_{i,t} - E_{i,t} - I_{i,t} - R_{i,t})] \frac{A_i}{A} \quad (4)$$

where $S_{i,t-1}$ is the storage state of an LID type i at time $t-1$ [mm], $F_{i,t}$ is the inflow from the contributing area of an LID type i at time t [mm/min], $E_{i,t}$ is the evaporation loss from an LID type i at time t [mm/min], $I_{i,t}$ is the infiltration loss from an LID type i at time t [mm/min], $R_{i,t}$ is the runoff from an LID type i at time t [mm/min] and Δt is the time step [min].

When assessing the storage behaviour of the alternative designs at the block scale the contributing area for each LID type i was also considered to account for the fact that it is not merely the water column storage depth (D_i) (Eq. (1)) that determines the LID efficiency. The contributing area ($A_{c,i}$) was defined by tracing the drainage network upstream from the subcatchment with an LID unit. Capture ratio of an LID type i ($C_{r,i}$) and capture ratio of stormwater management designs A-C ($C_{r,tot}$) at residential block scale were computed using Eqs. (5) and (6), respectively.

$$C_{r,i} = \frac{A_{c,i}}{A_i} \quad (5)$$

$$C_{r,tot} = \frac{\sum_{i=1}^n A_{c,i}}{\sum_{i=1}^n A_i} \quad (6)$$

2.4.2. Restoring natural hydrological behaviour

Runoff reductions due to stormwater losses, i.e., infiltration and evapotranspiration, were assessed for both individual LID types and for the residential block. The losses were studied separately for periods P1 and P2 to detect seasonal differences. In addition, the extent to which stormwater management at Kirstinpuisto catchment can help in restoring the natural hydrological behaviour was assessed by comparing runoff coefficients and model simulation results with flow measurements from two reference watersheds for the 7-month simulation period including P1 and P2 periods. For the Kirstinpuisto catchment, stormwater runoff was computed as the sum of simulated stormflow at the two outlets of the drainage network divided by the catchment areas. For the reference watersheds, runoff means measured streamflow divided by the watershed area. In the reference watersheds, including the semi-urban reference watershed, runoff therefore refers to flow in a stream or in an urban brook but not in the piped network. The runoff coefficient is the ratio of runoff depth to rainfall depth.

2.4.3. Sensitivity of outflow to LID investment costs

The cost efficiency of different LID types was expressed as stormwater runoff volume reduction per additional investment cost, defined as

$$E_{c,i} = \sum_{t=1}^T [(E_{i,t} + I_{i,t}) \Delta t] A_i / \epsilon_i \quad (7)$$

where $E_{c,i}$ [l/€] is the cost efficiency and the water balance components are the same as defined in Eq. (4), and ϵ_i is the investment cost for LID type i .

Sensitivity of stormwater outflow to investment costs associated with different LID setups was assessed by conducting model simulations for all possible LID combinations of either activating or deactivating planned LID units (*PP*, *GR* and *RG*) in design *C*. The subarea delineated by a red line in Fig. 3 was used for the sensitivity analysis. This resulted in 2 048 different LID combinations. *VS* was not included in the analysis as it serves as the conveyance structure directing stormwater away from the block area in all designs. Ideally one would sample all possible combinations for the entire block but this would have led to 262 143 model runs, which was deemed infeasible due to the computational burden.

3. Results

3.1. Storage capacity and dynamics

The block charts in Fig. 4 depict the LID specific storage capacity M_i computed using Eq. (2) for all LID types in the alternative stormwater management designs A-C at the residential block. M_i indicates the maximum capacity of an LID type i to store stormwater without consideration for the decreasing storage volume due to recharge from precipitation or for the inter-event recovery of the storage volume. *PP* covering almost the same area as *RG* in design *B* (Fig. 3) had three times larger specific storage capacity (Fig. 4), which was facilitated by the larger water column depth (D_i). In design *C*, *PP* with 7% smaller areal coverage had three times larger storage capacity than *GR*.

Fig. 4 shows the exceedance frequency for the dynamic storage (Eq. (4)). During the seven-month simulation period, the *GR* storage capacity was exhausted for ca. 20% of the time. For other LID structures exhaustion of storage capacity occurred only for very short time periods (*VS* and *RG* for design *A*, *RG*, *BC* and *PP* for design *B*, and *RG* for design *C*) or not at all (*VS* for design *B*, and *VS* and *PP* for design *C*). In fact, for most LID types the state of the dynamic storage remained predominantly well below the static capacity. Fig. 4 also reveals a clear change in the storage dynamics of *PP* between designs *B* and *C*, which can be attributed to the increase in capture ratio from design *B* to *C* (Table 4) and a consequent increase in stormwater inflow to *PP*. Regardless of the same capture ratio, *VS* had different maximum dynamic storage values for designs A-C due to the difference in the percentage of upstream LID coverage (Table 4).

For design *A*, *VS* demonstrated quick storage and inter-event recovery responses (Fig. 5a-b), consistently storing and losing stormwater within about 15 h. *RG* had a much slower storage and inter-event recovery responses compared to *VS*, eventually returning to the wilting point moisture content during P1. However, storage did not recover to the wilting point moisture content in P2 due to the reduced evapotranspiration rate in the autumn (Fig. 5a). The storage capacities of *VS* and *RG* were completely depleted in design *A* at the end of P1 (Fig. 5b).

BC, *GR* and *PP* in design *B* as well as *RG* and *GR* in design *C* exhausted their storage capacities after the intense event occurring at the end of P1 (Fig. 5d and f). However, *PP* still had about 39 mm of the 70 mm specific storage capacity (M_i) remaining at the end of P1 in design *C* (Figs. 4 and 5e). *GR* and *PP* in design *C* demonstrated similar storage and inter-event recovery responses prior to a significant rain event in early October (Fig. 5e). However, after the early October event, the responses for *GR* and *PP* were different primarily due to the lack of infiltration in the former and initiation of infiltration from the storage layer in the latter. Before October, in design *C* stormwater in *PP* was mostly stored in soil layer and lost to evapotranspiration as suggested by the receding limbs with slow depletion rates (Fig. 5e). This was also the case in design *B* with less storage capacity in *PP* until the intense end-of-August event, during which infiltration was initiated (Fig. 5c). *GR* remained close to saturation for both designs *B* and *C* during P2, as evapotranspiration was

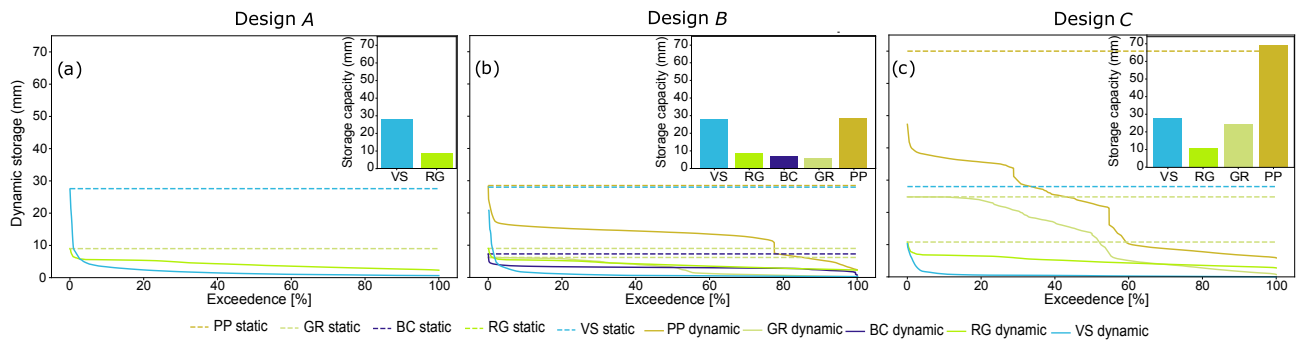


Fig. 4. The frequency of exceedance for storage values (solid line) for designs A (a), B (b) and C (c) at the residential block. Storage capacities are denoted with dashed lines. Bar charts indicate specific storage capacities for vegetated swale (VS), rain garden (RG), bioretention cell (BC), green roof (GR) and permeable pavement (PP). (For interpretation of the references to colour in this figure legend, the reader is referred to the web version of this article.)

Table 4

Capture ratio of LID type i ($C_{r,i}$), upstream LID coverage (A_{cvg}), capture ratio of designs ($C_{r,tot}$) and upstream LID coverage at the residential block scale (A_{tot}).

LID	VS		RG		BC		GR		PP		All LID types	
	$C_{r,i}$	A_{cvg} (%)	$C_{r,tot}$	A_{tot} (%)								
Design A	6.13	11.5	0.7	0	-	-	-	-	-	-	3.66	24
Design B	6.13	33.5	0.7	0	8.52	1.8	0	0	2.1	4.5	2.72	50
Design C	6.13	78.4	1.2	9.7	-	-	0	0	1.29	37.9	1.52	92

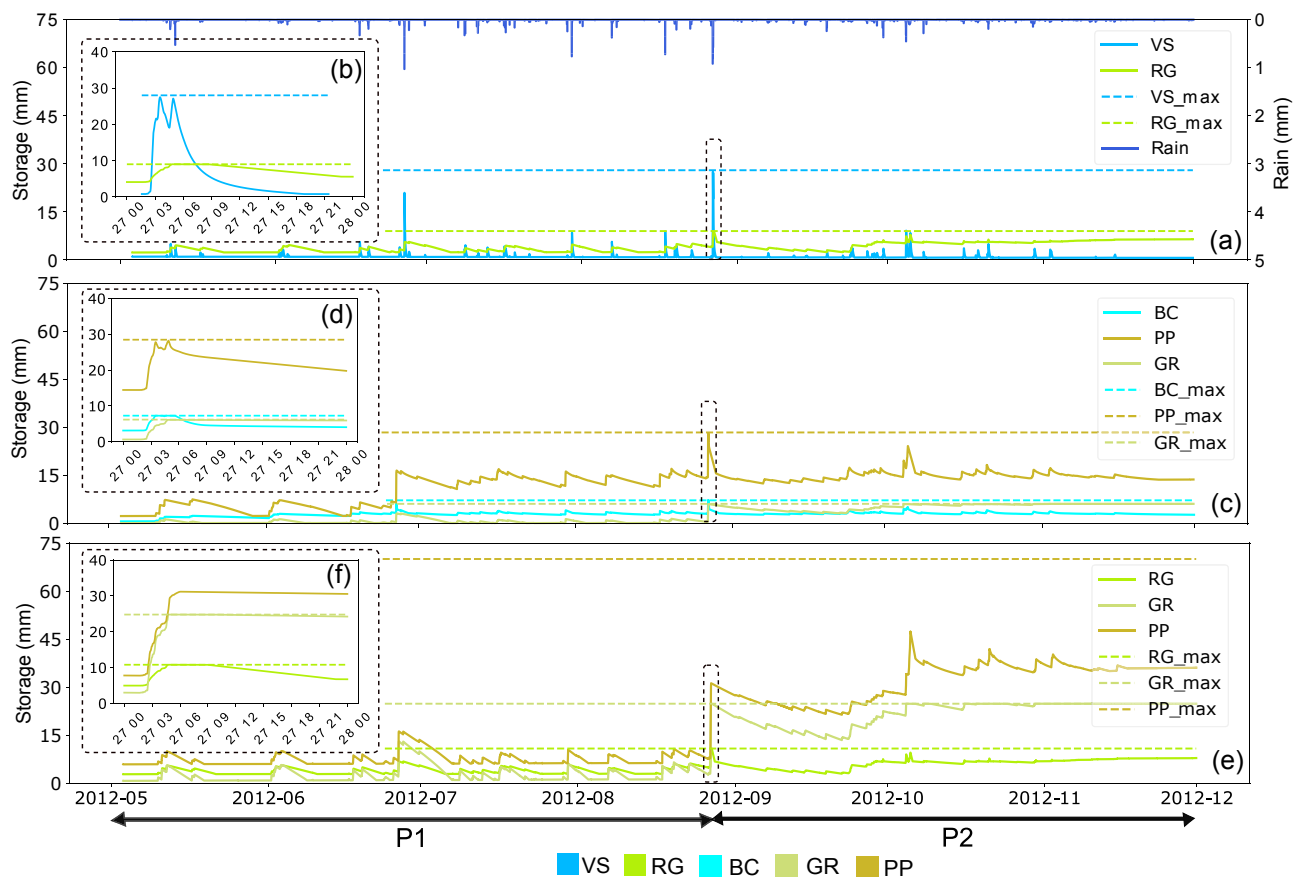


Fig. 5. Time series of dynamic storage for selected LID types in design A (a and b), design B (c and d) and design C (e and f) during the seven-month simulation period at the residential block scale (a, c, e). The black dotted box shows storage dynamics during 27 August 2012 for all designs (b, d, and f). Coloured dotted lines show the maximum storage capacity for each LID. P1 and P2 mark summer and autumn periods. The horizontal axis in (a), (c) and (e) show year-month and (b), (d) and (f) show day-hour values.

reduced during colder months (Fig. 5c and e).

3.2. Restoring natural hydrological behaviour

Fig. 6 shows the stormwater runoff depth reduction by LID types due to infiltration and evapotranspiration for P1 and P2 at the residential block scale. In P1, stormwater runoff reduction was dominated by evapotranspiration for all LID types except for VS and BC, where infiltration was prominent. The larger evapotranspiration for GR and PP in design C when compared to design B is explained by the larger LID specific storage capacity (Fig. 4). When moving from P1 to P2, the mechanism of stormwater runoff reduction shifted towards infiltration for all LID types except for GR and VS due to the reduced evapotranspiration during colder months. Stormwater runoff reduction for VS was infiltration dominated in both periods, and for GR resulted solely from evapotranspiration due to the lack of infiltration capacity. Since the area of LIDs upstream of VS increased from design A to C, the stormwater inflow to VS decreased leaving less water for infiltration.

The extent to which stormwater runoff reduction by alternative stormwater management designs at catchment scale restores the natural hydrological behaviour was studied by comparing runoff coefficients (Table 5) and cumulative plots of runoff depths at the outlets of the Kirstinpuisto catchment and the two reference watersheds (Fig. 7).

Stormwater runoff coefficients decreased from designs A to B to C for both summer P1 and autumn P2 periods due to the increasing coverage of LID types facilitating disconnection of the impervious area from the drainage network (Table 5). During P1, stormwater runoff coefficients for designs B and C closely resembled runoff coefficients of the semi-urban and rural reference watersheds, respectively. However, there was no resemblance of runoff coefficients between designs B and C and reference watersheds during P2. Interestingly, the stormwater runoff coefficient of design A with an imperviousness of 70% was comparable to the runoff coefficient of the semi-urban reference watershed with an imperviousness of 24% during P2.

The simulated stormwater runoff depths for designs B and C (Fig. 7a) accumulated gradually compared to the steep slopes of the measured runoff depths of the reference watersheds during autumn period P2. This was because the amount of water infiltrating into the underlying soil was higher during autumn (P2) compared to summer period (P1) for designs A-C (see Fig. 6a and 6c). The infiltrated water did not appear as stormflow in the drainage network for designs A-C, although in the reference watersheds some of it eventually emerges as streamflow

Table 5

Stormwater runoff coefficients in the management designs A-C, and runoff coefficients for generation of streamflow in the reference watersheds during P1 and P2.

Designs	P1	P2
Design A	0.49	0.42
Design B	0.31	0.24
Design C	0.10	0.06
Semi-urban reference (Kuninkoja)	0.24	0.51
Rural reference (Savijoki)	0.10	0.60

(Fig. 7a). However, when the sum of the simulated stormwater runoff and infiltration was compared against the measured runoff of the reference watersheds (Fig. 7b), the autumn accumulation of the Kirstinpuisto catchment also became steeper resembling more the shape of the reference watersheds. Design C with the largest contribution to evapotranspiration (Fig. 6b and d), and lowest imperviousness of 23%, produced now an accumulation curve closely resembling the flow dynamics of the reference semi-urban watershed with an imperviousness of 24% (Fig. 7b).

Adopting cumulative runoff plots as a vehicle of comparison rather than the often-used flow frequency curves was motivated by the large discrepancy between catchment sizes in Kirstinpuisto and reference areas. A smaller catchment is more prone to produce small and large runoff values than a larger catchment where baseflow plays a role and there is more lag in the system, which would lead to different flow frequency curves merely due to catchment size discrepancies. Cumulative runoff depth curves (Fig. 7) provide a more robust basis for runoff comparison between differently sized catchments as they integrate runoff values from a longer time rather than focus on snapshots of momentary flow values. Transition to wet state occurs later in the rural Savijoki than in the semi-urban Kuninkoja watershed. This is explained by a higher moisture deficit created by summer evapotranspiration in the former. The larger moisture deficit can be seen as a delayed initiation of autumn runoff despite autumn rains and decreasing evapotranspiration.

Groundwater flow was not simulated in this study. While activation of the SWMM groundwater module could affect the proportions of computed stormwater flow and infiltration, there is no reason to assume that the sum of the two would significantly change. In fact, even the proportions are unlikely to change as SWMM groundwater module does not allow lateral movement of groundwater between subcatchments and

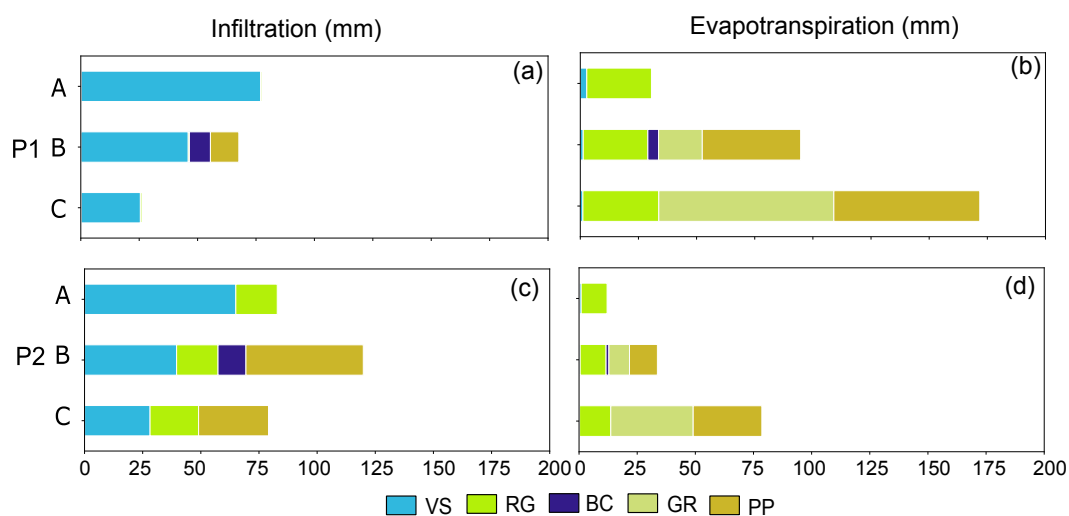


Fig. 6. Infiltration and evapotranspiration for simulation periods P1 (a and b) and P2 (c and d) at the residential block scale for designs A-C. VS, RG, BC, GR and PP refer to vegetated swale, rain garden, bioretention cell, green roof and permeable pavement, respectively. (For interpretation of the references to colour in this figure legend, the reader is referred to the web version of this article.)

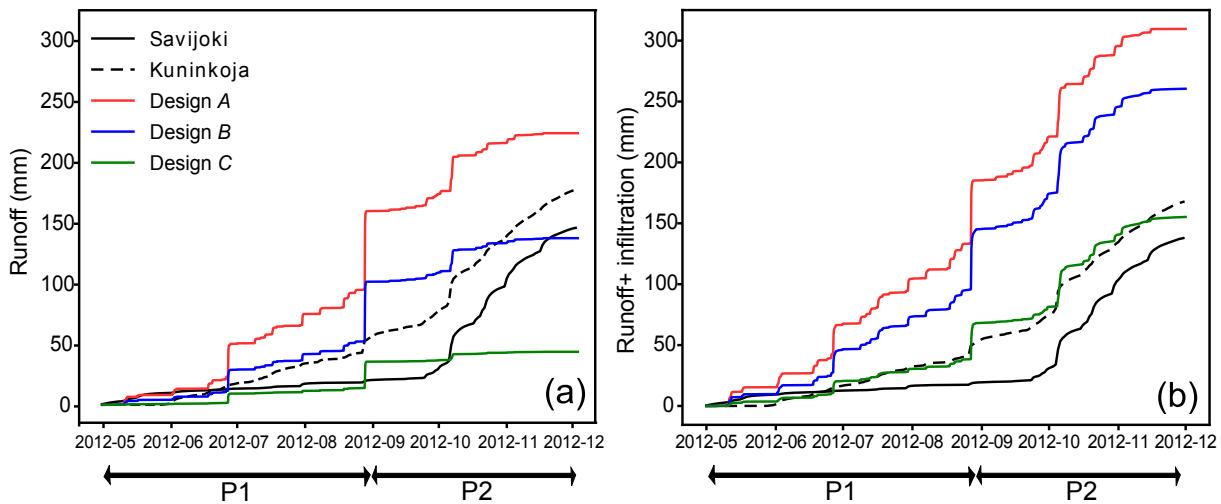


Fig. 7. Cumulative runoff depths for stormwater management designs A-C at catchment scale against runoff depths of the reference watersheds (a). Cumulative sum of runoff and infiltration for the studied designs against runoff depths of the rural reference (Savijoki) and semi-urban reference (Kuninkoja) watersheds (b).

most of the vegetated areas do not have stormwater pipes which could receive water when groundwater table rises above the drain level.

3.3. Sensitivity of outflow to LID investment costs

Fig. 8 compares the efficiency of LID types in designs A-C to reduce stormwater runoff volume via infiltration and evapotranspiration per unit cost. The cost efficiency of LID types is computed according to Eq. (7). When comparing VS and RG for design A, VS was the more cost-efficient type at reducing stormwater volume. In design B, BC was the most cost-efficient type. Although the investment cost for BC was almost twice that of PP (Table 3), the cost efficiency of BC in reducing stormwater volume was higher because of a higher capture ratio of BC (Table 4). The cost efficiency of VS with a constant capture ratio of 6.1 in all designs decreases from A to B to C (Fig. 8) due to the increasing percentage of LID coverage upstream of VS (Table 4). RG, having a relatively low capture ratio (Table 4) but bearing a low investment cost

(Table 3) was the second cost-efficient LID type in design B and the most cost-efficient LID type in design C.

Results depicting the impact of LID setup on investments costs (Fig. 9) show that for design C there was no runoff from the block subarea used in the analysis (Fig. 3). The entire block generated a small amount of runoff (26 mm), originating mainly from the southern bank of the swale. It is evident that design C (blue square in Fig. 9) was overly intensive as negligible runoff was also achieved with a design alternative having a smaller number of LID units and bearing a lower investment cost (e.g. brown square in Fig. 9).

The large jump in the runoff reduction between ellipses E1 and E2 (Fig. 9) was attributed to the activation of PP numbered 4 and RG numbered 2 (Fig. 3). These two structures alone provided a cost-efficient setup by greatly reducing runoff at a modest additional cost (magenta square in Fig. 9). The pronounced role of these units is explained by their large treatment area, i.e. the sum of their own area and the contributing area. The rain garden has a large capture ratio of 6.6 while its own area is relatively small (80 m²). The permeable pavement has a large area (1420 m²) and a capture ratio of 2.1. The combined treatment area for these two units is 5800 m², which is 42% of the area used in the sensitivity analysis.

4. Discussion

4.1. Storage capacity and dynamics

The static storage approach (Fig. 4, Eqs. (2) and (3)) serves as a simple performance evaluation criterion that can be easily discerned already during the design phase from the physical characteristics and areal coverage of LID structures. This approach was adopted in several earlier studies to evaluate the performance of LID types in reducing peak flow, runoff volume, and occurrence of flooding (Guan et al., 2015a; Qin et al., 2013; Walsh et al., 2014). However, LID designs based on static storage capacity can overestimate the retention capacity at the onset of a rain event because the initial volume of water stored in LID structures is not accounted for.

In contrast to the static storage approach, the dynamic storage approach involving continuous simulations over several months provided information to understand the inter-event restoration of LID storage capacity through stormwater losses. As can be seen from storage exceedance curves (Fig. 4), the amount of available storage can be significantly smaller than the capacity for prolonged periods, and for some LID types the capacity is occasionally exceeded. On the other hand, despite the fact that the available storage is smaller than the capacity,

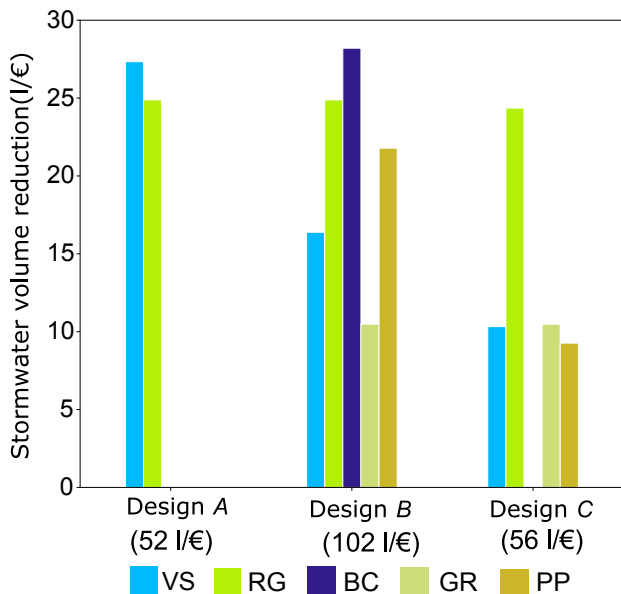


Fig. 8. Efficiency of LID types in reducing stormwater volume via infiltration and evapotranspiration per unit cost for designs A-C at residential block scale for the seven-month simulation period. The values below labels Design A-C denote the total efficiencies across those designs.

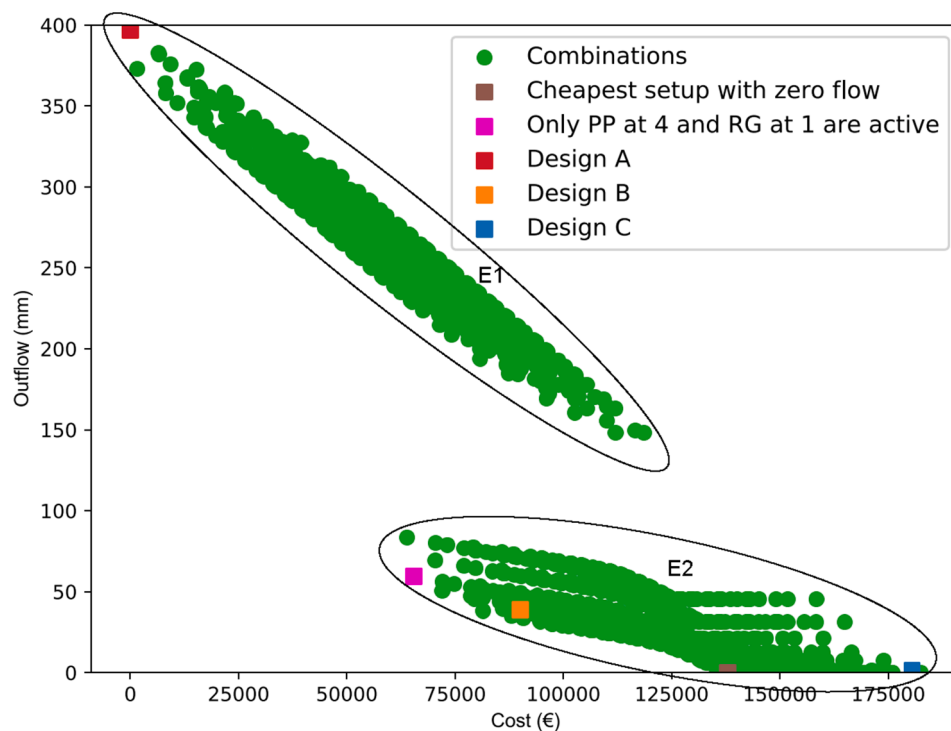


Fig. 9. Relation between stormwater runoff (Outflow) and investment costs associated with LID setups (Cost) for all combinations of alternatively activating or deactivating LID units in design C. Results for designs A, B and C are indicated as squares. PP at 4 and RG at 1 refer to the numbered LID units in Fig. 3. Activation of these two LID units splits the plot to ellipses E1 and E2.

for nearly all LID types the state of the dynamic storage is most of the time well below the static capacity. Modelling is one way to explore whether planned LID dimensions dictating the static storage capacity are sufficient but not excessive. Jia et al. (2012) studied LID designs for the Beijing Olympic Village and suggested decreased dimensions for LID structures after optimization when compared to initial designs.

The results of long-term SWMM simulations depicted how storage capacity recovery of LID types was highly influenced by the seasonal differences in weather controlling infiltration and evapotranspiration rates. SWMM-LID module, however, has been shown to suffer from uncertainties in describing the storage recovery. Platz et al. (2020) found out that particularly for deep LID types SWMM was prone to underestimate outflow due to its inability to account for lateral flow into the soil at the sides of the structure. Baek et al. (2020) coupled SWMM with HYDRUS-1D model, which lead to improved accuracy in simulation of green roof soil moisture and outflow from an urban catchment. Despite these inherent uncertainties in SWMM-LID module, it still represents the state-of-the-art that has been widely adopted by researchers and environmental consultants.

4.2. Restoring natural hydrological behaviour

The sum of computed stormwater runoff and infiltration resembled more closely the reference watershed flow measurements (Fig. 7b) than the computed stormwater runoff alone (Fig. 7a). Evidently, runoff in streams draining urban areas has been conveyed either via the fast responding stormwater drainage network or through a slower soil water route. The split between these two routes is affected by the connectivity of urban surfaces with the pipe network and by the season. These findings are consistent with the results presented by Walsh et al. (2012) and Bonneau et al. (2018). The former reported decreased baseflow in receiving urban streams for conventionally drained urban areas in comparison with areas with informal drainage to adjacent permeable areas. The latter noticed distinct seasonality with a higher share of infiltrated stormwater reaching an urban stream over the autumn

season. Consequently, the results of this study support the view that it is arguable how restoration of the natural flow regime can be evaluated using only stormwater network measurements.

When the goal is to mimic the undeveloped flow regime, care needs to be taken when designing LID types. Restoring hydrological regime of an urban area requires bringing the evapotranspiration rates back to the undeveloped conditions (design C in Figs. 6 and 7b). Otherwise, there can even be the risk to ‘overcompensate’ by increasing the amount of infiltration, and hence baseflow, to exceed the undeveloped state by reducing evapotranspiration and conveying stormwater from impervious surfaces to infiltration based LID structures (Bhaskar et al. 2016).

4.3. Sensitivity of outflow to LID investment costs

Results presented here showed that the capture ratio, i.e., the ratio of the contributing area to the area covered by an LID type, the recovery rate of storage capacity, the associated investment costs, and the percentage of upstream LID coverage were essential in defining the cost efficiency of an LID type. Bioretention cell (BC) with the largest capture ratio followed by rain garden (RG) with the smallest associated investment costs and permeable pavement (PP) in design B with the highest storage capacity were the most cost-efficient LID types (Fig. 8). The cost efficiency of the vegetated swale at the downstream end of the treatment train decreased with the increasing upstream LID coverage. This is neither visible for rain garden nor for green roofs (GR). RG areas are mostly located on the southern bank of the swale with no contributing upstream area, and green roofs are at the upstream end of the treatment train with no contributing area. While GR has a relatively modest cost efficiency compared to other structures, it is worth noting that GR can be a viable type in densely constructed areas, where space is limiting construction of other types of LID structures (Hamouz et al., 2020). Huang et al. (2018) identified GR, along with BC, as the main components in their cost-benefit analysis for the optimal design to mitigate urban flooding in Taipei.

Investigation of the LID impacts on streamflow when alternatively

activating and deactivating LID units revealed the most efficient units within the study region. Activating the two most influential LID units having a high storage capacity and a capture ratio – one permeable pavement (storage capacity: 28 mm) and one rain garden (capture ratio: 6.6) – lead to a drastic drop in stormwater outflow with a relatively low investment cost (Fig. 9). From the tested designs A, B and C the most intensive design C is overly intensive as the same impact on stormwater outflow could be achieved at a considerably lower cost. Jia et al. (2012) reported decreased dimensions for LID structures following an optimization with regard to LID costs.

The results showed that a treatment train requiring the minimal cost, i.e. design A, was not the most cost efficient (Fig. 8) because runoff reduction was the smallest (Fig. 7). In addition, the large capture ratios of LID types in design A may result in high inflows leading to clogging and increased operation costs. Cost evaluation throughout the lifecycle, including operation and maintenance costs, is evidently essential (Liu et al., 2014). However, earlier cost efficiency studies based on realistic construction, operation and maintenance costs for LID types have shown inconsistent results due to differences in local contexts, system designs, and analysis boundaries (e.g. Bixler et al., 2020; Chui et al., 2016). The operation and maintenance costs (OMC) are further affected by the assumed lifespan of the LID types. The assumed average lifespan of LID types varies between 15 years (Huang et al., 2018) and 50 years (Ossa-Moreno et al., 2017) with 30 year being the commonly used average lifespan (Chui et al. 2016). This results in OMC estimations ranging from 1.5 % of the initial investment costs (Joshi et al., 2021) up to 19 % (Houle et al., 2013). While a comprehensive lifecycle cost evaluation would be optimal, it is clearly complex, case specific, and poorly transferable to other regions and therefore outside the scope of this research.

This study focused on investment costs for decreasing stormwater flow volumes using combinations of LID types. Yang and Chui (2018) applied a large set of SWMM simulations to optimize areal coverage of bioretention cells (BC) and their capture areas. In addition to reducing runoff volume, they included the decrease of peak flow and the first flush flow volume as optimization criteria. The most efficient BC designs were efficient for flow volume control but the efficiency varied for reducing intensive peak flows. Results from Yang and Chui (2018) and from the current study suggest that with a moderate coverage of critical LID types, a part of the natural retention and detention functions can be restored when evaluated in terms of the flow volume control.

5. Conclusions

To facilitate the adoption of LID types, it is necessary to provide methods for their quantitative performance evaluation. This study highlights that dynamic performance evaluation based on long-term simulations conducted already during the design phase can prove essential in assessing efficiencies of LID types.

Dynamic LID storage assessment, in contrast to the static storage approach, accounts for infiltration and evapotranspiration fluxes and incorporates storage restoration rate into the LID performance evaluation. The main benefit of the dynamic storage approach is the realistic estimation of runoff volume reduction via infiltration and evapotranspiration compared to dimensioning LID structures using the size of the static storage alone. The static storage approach can lead to non-optimal LID dimensioning, which was seen as too large capacities for most LID types in this study. To improve the design of LID types, it is important to incorporate storage restoration rate in the design process through continuous simulations extending over several months.

The simulations together with reference data enable comparing the resemblance of the flow regime of the constructed area to its more natural counterparts. In small urban catchments, use of stormflow alone can be misleading when comparing the flow regime to the undeveloped state. Infiltrated water can also eventually emerge as a flow in the receiving stream without ever entering the stormwater drainage

network. Simple comparison of the volume of piped stormflow with volume of gauged natural streamflow can lead to misleading results.

The main benefit of arranging LID types in a treatment train is the augmented stormwater volume reduction facilitated by efficient utilization of the available storage capacity as overflowing water from one LID unit is treated by the next unit in the chain. A treatment train with either a small storage capacity or a small capture ratio can have a limited stormwater reduction resulting in lower cost efficiency compared to the train where storage capacity and capture ratio are in balance. An extensive simulation of a large set of differently placed LID units within a treatment train provides an attractive way to identify those critical units that yield the most cost-efficient LID design.

CRediT authorship contribution statement

Ambika Khadka: Conceptualization, Methodology, Software, Visualization, Writing - original draft. **Teemu Kokkonen:** Conceptualization, Supervision, Writing - review & editing. **Harri Koivusalo:** Conceptualization, Writing - review & editing. **Tero J. Niemi:** Writing - review & editing. **Piia Leskinen:** Investigation, Writing - review & editing. **Jan-Hendrik Körber:** Investigation, Writing - review & editing.

Declaration of Competing Interest

The authors declare that they have no known competing financial interests or personal relationships that could have appeared to influence the work reported in this paper.

Acknowledgements

This work was funded by Ministry of Agriculture and Forestry, Finland; Schlumberger Foundation Faculty for the Future, Academy of Finland (no 326787, WaterWorks2017 ERA-NET Cofund) and Maa- ja vesitekniiikan Tuki ry. The study was part of the UrbanStormwaterRisk and EviBAN (Evidence based assessment of NWRM for sustainable water management) projects. Elisa Lähde, a landscape architect, designed the alternative stormwater management designs assessed in this study. The rainfall data for design simulations came from a rain gauge operated by the City of Turku. The streamflow data for rural reference watershed (Savijoki) and semi-urban reference watershed (Kuminkoja) came from monitoring stations maintained by the Finnish Environment Institute (SYKE) and Turku University of Applied Sciences (TUAS), respectively.

References

- Avellaneda, P.M., Jefferson, A.J., Grieser, J.M., Bush, S.A., 2017. Simulation of the cumulative hydrological response to green infrastructure. *Water Resour. Res.* 53 (4), 3087–3101. <https://doi.org/10.1002/2016WR019836>.
- Baek, S., Ligaray, M., Pachepsky, Y., Chun, J.A., Yoon, K.-S., Park, Y., Cho, K.H., 2020. Assessment of a green roof practice using the coupled SWMM and HYDRUS models. *J. Environ. Manage.* 261, 109920. <https://doi.org/10.1016/j.jenvman.2019.109920>.
- Behörde für Stadtentwicklung und Umwelt Freie und Hansestadt Hamburg, 2006. Dezentrale naturnahe Regenwasserbewirtschaftung [WWW Document].
- Bhaskar, A.S., Hogan, D.M., Archfield, S.A., 2016. Urban base flow with low impact development. *Hydro. Process.* 30 (18), 3156–3171. <https://doi.org/10.1002/hyp.v30.1810.1002/hyp.10808>.
- Bixler, T.S., Houle, J., Ballesteros, T.P., Mo, W., 2020. A spatial life cycle cost assessment of stormwater management systems. *Sci. Total Environ.* 728, 138787. <https://doi.org/10.1016/j.scitotenv.2020.138787>.
- Bonneau, J., Fletcher, T.D., Costelloe, J.F., Poelsma, P.J., James, R.B., Burns, M.J., 2018. Where does infiltrated stormwater go? interactions with vegetation and subsurface anthropogenic features. *J. Hydrol.* 567, 121–132. <https://doi.org/10.1016/j.jhydrol.2018.10.006>.
- Chui, T.F., Liu, X., Zhan, W., 2016. Assessing cost-effectiveness of specific LID practice designs in response to large storm events. *J. Hydrol.* 533, 353–364. <https://doi.org/10.1016/j.jhydrol.2015.12.011>.
- CORINE, 2018. CORINE Land Cover - Copernicus Land Monitoring Service [WWW Document]. Copenhagen, Denmark Eur. Environ. Agency. URL <https://land.copernicus.eu/pan-european/corine-land-cover/clc2018>.
- DWA, 2014. DWA Set of Rules Standard DWA-A 272E: Planning for the Planning and Implementation of New Alternative Sanitation Systems (NASS) [WWW Document].

- Ebrahimian, A., Wadzuk, B., Traver, R., 2019. Evapotranspiration in green stormwater infrastructure systems. *Sci. Total Environ.* 688, 797–810. <https://doi.org/10.1016/j.scitotenv.2019.06.256>.
- EEA, 2018. Copernicus Land Monitoring Service-High Resolution Layers-Imperviousness [WWW Document]. Copenhagen, Denmark Eur. Environ. Agency. URL <https://www.eea.europa.eu/data-and-maps/data/copernicus-land-monitoring-service-imperviousness-2>.
- Guan, M., Sillanpää, N., Koivusalo, H., 2015a. Assessment of LID practices for restoring pre-development runoff regime in an urbanized catchment in Southern Finland. *Water Sci. Technol.* 71 (10), 2015–2017. <https://doi.org/10.2166/wst.2015.129>.
- Guan, M., Sillanpää, N., Koivusalo, H., 2015b. Modelling and assessment of hydrological changes in a developing urban catchment. *Hydrol. Process.* 29 (13), 2880–2894. <https://doi.org/10.1002/hyp.v29.1310.1002/hyp.10410>.
- Haghighatafshar, S., la Cour Jansen, J., Aspegren, H., Jönsson, K., 2018. Conceptualization and schematization of mesoscale sustainable drainage systems: a full-scale study. *Water (Switzerland)* 10 (8), 1041. <https://doi.org/10.3390/w10081041>.
- Hamouz, V., Møller-Pedersen, P., Muthanna, T.M., 2020. Modelling runoff reduction through implementation of green and grey roofs in urban catchments using PCSWMM. *Urban Water J.* 17 (9), 813–826. <https://doi.org/10.1080/1573062X.2020.1828500>.
- Houle, J.J., Roseen, R.M., Ballesterio, T.P., Puls, T.A., Sherrard, J., 2013. Comparison of maintenance cost, labor demands, and system performance for LID and conventional stormwater management. *J. Environ. Eng.* 139 (7), 932–938. [https://doi.org/10.1061/\(ASCE\)EE.1943-7870.0000698](https://doi.org/10.1061/(ASCE)EE.1943-7870.0000698).
- Huang, C.L., Hsu, N.S., Liu, H.J., Huang, Y.H., 2018. Optimization of low impact development layout designs for megacity flood mitigation. *J. Hydrol.* 564, 542–558. <https://doi.org/10.1016/j.jhydrol.2018.07.044>.
- Jefferson, A.J., Bhaskar, A.S., Hopkins, K.G., Fanelli, R., Avellaneda, P.M., McMillan, S. K., 2017. Stormwater management network effectiveness and implications for urban watershed function: a critical review. *Hydrol. Process.* 31 (23), 4056–4080. <https://doi.org/10.1002/hyp.v31.2310.1002/hyp.11347>.
- Jia, H., Lu, Y., Yu, S.L., Chen, Y., 2012. Planning of LID-BMPs for urban runoff control: the case of Beijing Olympic Village. *Sep. Purif. Technol.* 84, 112–119. <https://doi.org/10.1016/j.seppur.2011.04.026>.
- Joksimovic, D., Alam, Z., 2014. Cost efficiency of Low Impact Development (LID) stormwater management practices, in: *Procedia Engineering*. Elsevier Ltd, pp. 734–741. [10.1016/j.proeng.2014.11.501](https://doi.org/10.1016/j.proeng.2014.11.501).
- Joshi, P., Leitão, J.P., Maurer, M., Bach, P.M., 2021. Not all SuDS are created equal: Impact of different approaches on combined sewer overflows. *Water Res.* 191, 116780. <https://doi.org/10.1016/j.watres.2020.116780>.
- Khadka, A., Kokkonen, T., Niemi, T.J., Lähde, E., Sillanpää, N., Koivusalo, H., 2019. Towards natural water cycle in urban areas: modelling stormwater management designs. *Urban Water J.* 17 (7), 587–597. <https://doi.org/10.1080/1573062X.2019.1700285>.
- Leimgruber, J., Krebs, G., Camhy, D., Muschalla, D., 2019. Model-based selection of cost-effective low impact development strategies to control water balance. *Sustain* 11 (8), 2440. <https://doi.org/10.3390/su11082440>.
- Liu, J., Sample, D., Bell, C., Guan, Y., 2014. Review and research needs of bioretention used for the treatment of urban stormwater. *Water (Switzerland)* 6 (4), 1069–1099. <https://doi.org/10.3390/w6041069>.
- Manfred, K., 2012. *Handbuch Bauwerksbegrünung Planung – Konstruktion – Ausführung*. Verlagsgesellschaft Rudolf Müller GmbH & Co. KG, Dach, Fassade, Innenraum.
- Ossa-Moreno, J., Smith, K.M., Mijic, A., 2017. Economic analysis of wider benefits to facilitate SuDS uptake in London, UK. *Sustain. Cities Soc.* 28, 411–419. <https://doi.org/10.1016/j.scs.2016.10.002>.
- Platz, M., Simon, M., Tryby, M., 2020. Testing of the storm water management model low impact development modules. *J. Am. Water Resour. Assoc.* 56 (2), 283–296. <https://doi.org/10.1111/jawr.v56.210.1111/1752-1688.12832>.
- Qin, H.-p., Li, Z.-xi., Fu, G., 2013. The effects of low impact development on urban flooding under different rainfall characteristics. *J. Environ. Manage.* 129, 577–585. <https://doi.org/10.1016/j.jenvman.2013.08.026>.
- Rossmann, L.A., Huber, W.C., 2016. Storm water management model reference manual volume I – hydrology. U.S. Environ. Prot. Agency I 233. [https://doi.org/10.1016/S0021-9290\(00\)00018-X](https://doi.org/10.1016/S0021-9290(00)00018-X).
- Sarkkola, S., Nieminen, M., Koivusalo, H., Lauren, A., Ahti, E., Launiainen, S., Nikinmaa, E., Marttila, H., Laine, J., Hökkä, H., 2013. Domination of growing-season evapotranspiration over runoff makes ditch network maintenance in mature peatland forests questionable. *Mires Peat* 11, 1–11.
- Sillanpää, N., 2013. Effects of suburban development on runoff generation and water quality. Aalto Univ. Publ. Ser. Dr. Diss. 160/2013.
- Tahvonen, O., 2018. Adapting bioretention construction details to local practices in Finland. *Sustain.* 10 (2), 276. <https://doi.org/10.3390/su10020276>.
- Traver, R.G., Ebrahimian, A., 2017. Dynamic design of green stormwater infrastructure. *Front. Environ. Sci. Eng.* 11 (4) <https://doi.org/10.1007/s11783-017-0973-z>.
- Turunen, M., 2017. Assessing water and sediment balances in clayey agricultural fields in high latitude conditions. Aalto Univ. Publ. Ser. Dr. Diss. 67 (2017), 173.
- Walsh, C.J., Fletcher, T.D., Burns, M.J., Gilbert, J.A., 2012. Urban stormwater runoff: a new class of environmental flow problem. *PLoS ONE* 7 (9), e45814. <https://doi.org/10.1371/journal.pone.0045814>.
- Walsh, T.C., Pomeroy, C.A., Burian, S.J., 2014. Hydrologic modeling analysis of a passive, residential rainwater harvesting program in an urbanized, semi-arid watershed. *J. Hydrol.* 508, 240–253. <https://doi.org/10.1016/j.jhydrol.2013.10.038>.
- Yang, Y., Chui, T.F.M., 2018. Optimizing surface and contributing areas of bioretention cells for stormwater runoff quality and quantity management. *J. Environ. Manage.* 206, 1090–1103. <https://doi.org/10.1016/j.jenvman.2017.11.064>.